Journal of Thermal Science Vol.31, No.6 (2022) 1970−1989

https://doi.org/10.1007/s11630-022-1649-y **Article ID: 1003-2169(2022)06-1970-20**

Heat Transfer Model Founded and Regional Suitability Analysis of Photovoltaic Walls with Different Structures

ZHANG Wenjie[1*], ZHAO Yingbo[1], LIU Wei[2], GONG Tongdan[1], LIU Kangyong[1]

1. School of Energy and Power Engineering, Nanjing University of Science and Technology, Nanjing 210094, China
2. China Construction Sixth Division Construction & Development Co. Ltd., Tianjin 300451, China

Abstract: The heat transfer performance and suitability of photovoltaic walls with different structures in different regions have been studied. First, a quasi-two-dimensional calculation model was established to realize the simulation of photovoltaic walls with three structural forms (ordinary wall with air layer opening, air layer closed and no air layer); combined with the experimental data, the accuracy of the two-dimensional calculation model was verified. Based on the simulation results, the suitability of different structural forms of photovoltaic walls in areas with different climatic conditions were compared and analyzed. The results of the study show that the southern China that emphasize the purpose of ventilation and heat dissipation should adopt photovoltaic walls with open air layers, and the northern regions that emphasize the purpose of heat preservation and heat insulation should adopt photovoltaic walls with closed air layers; for transitional areas, the type of photovoltaic wall should be considered comprehensively according to environmental conditions and local building conditions.

Keywords: photovoltaic wall, thermal performance, numerical simulation, regional suitability

1. Introduction

Solar energy is currently the most widely-distributed and resource-abundant renewable energy in the world. Solar photovoltaic power generation technology is one of the utilization forms of solar energy. In the current situation of oil, carbon and other energy shortages, solar energy has received extensive attention from various research [1–3]. Countries have stepped up the pace of development of photovoltaics. Under the background of China's efforts to reach the peak of carbon dioxide emissions before 2030 and to achieve carbon neutrality before 2060, photovoltaic has shown broad development prospects [4] in the transformation of energy structure, especially in the field of building energy saving. The development potential of photovoltaic (PV) technology is immeasurable.

As an important technical means of building energy saving, PV wall has been widely used in daily production and life. The PV wall combined with the building facade can not only save the expensive floor space, but also reduce the carbon dioxide emission and energy use of the building [5, 6]. Therefore, it has become an important research direction to improve the performance of PV wall and explore the universality of PV wall in different areas. Domestic and foreign scholars have done a lot of research work on PV wall. Gao Feng [7] proposed a PV wall structure with ventilated flow channels. The design leaves a gap between the solar photovoltaic panel and the wall and achieves mechanical ventilation and heat

Special column: Built Thermal Environment GE: ZHAO Xudong
Received: May 21, 2021 AE: FAN Liwu Corresponding author: ZHANG Wenjie E-mail: zhangwenjie001@139.com

Nomenclature

A	the PV module area/m^2	T_{inlet}	inlet temperatures of the air layer respectively/K
A_i	the area in the vertical direction of the unit/m^2	T_{outlet}	outlet temperatures of the air layer respectively/K
C_{air}	the specific heat capacity of air/$J\cdot kg^{-1}\cdot K^{-1}$	$T_{inlet,i}$	the inlet temperature of the control unit/K
C_{PV}	the specific heat capacity of the PV module/ $J\cdot kg^{-1}\cdot K^{-1}$	$T_{outlet,i}$	the outlet temperature of the control unit/K
C_{wall}	the specific heat capacity of the wall/$J\cdot kg^{-1}\cdot K^{-1}$	$T_{PV,in}$	the internal surface temperature of the PV module/K
EPS	Expanded Polystyrene	$T_{PV,out}$	the outer surface temperature of the PV module/K
G	the solar radiation intensity per unit area of the PV module/$W\cdot m^{-2}$	$T_{roomair}$	the indoor temperature, as the initial input parameter/K
$h_{PV,in}$	the convective heat transfer coefficients of the inner surfaces of the PV module/$W\cdot m^{-2}\cdot K^{-1}$	$T_{roomsurface}$	the surface temperature of other walls and objects in the room/K
$h_{PV,out}$	the convective heat transfer coefficients of the outer surfaces of the PV module/$W\cdot m^{-2}\cdot K^{-1}$	α_{PV}	the absorption rate of the PV module
$h_{wall,in}$	the heat transfer coefficient between the inner surface of the wall and the indoor air/ $W\cdot m^{-2}\cdot K^{-1}$	β_{PV}	the surface reflectivity of the PV module
$h_{wall,out}$	the convective heat transfer coefficient between the air layer and the outer surface of the wall/ /$W\cdot m^{-2}\cdot K^{-1}$	σ	the Stefan-Boltzmann constant, 5.67×10^{-8} $W/(m^2\cdot K^4)$
M_{wall}	the quality of the wall/kg	$\varepsilon_{PV,in}$	the emissivity of the inner surface of the PV module
p_e	the power output per unit area of the photovoltaic module/$W\cdot m^{-2}$	$\varepsilon_{PV,out}$	the emissivity of the outer surface of the PV module
$Q_{PV,out}$	the long-wave radiation loss item on the outer surface of the PV module/W	$\varepsilon_{wall,in}$	the emissivity of the inner surface of the wall
T_{airgap}	the air layer temperature/K	$\varepsilon_{wall,out}$	the emissivity of the outer surface of the building wall
$T_{amb.}$	the outdoor air temperature/K		

dissipation in summer through a crossflow fan. By comparing the heat dissipation of the south exterior wall of the room with wind and solar energy and that of the room with ordinary wall, it is found that the ventilation PV wall has better heat dissipation effect than that of the ordinary wall only when the outdoor temperature is high and the solar radiation intensity is strong, but the heat dissipation effect is worse when the outdoor temperature is low and there is no solar radiation.

Based on the limitations of traditional building integrated photovoltaic (BIPV) systems, Luo [8] proposed a prototype of building integrated photovoltaic thermoelectric (BIPVTE) wall system by combining the thermoelectric radiation system with photovoltaic modules (PV modules), and carried out numerical simulation research on different cities in hot summer and cold winter regions. The results show that the cooling effect of BIPVTE wall system on the inner surface of the envelope is more obvious either in summer or in winter. Taking the massive wall as a reference, BIPVTE wall can save 102.6% of the indoor air conditioning energy consumption on the hottest day in summer and only 12% of the indoor air conditioning energy consumption on the coldest day in winter, which is related to the thermal bridge effect.

In order to solve the problem of low electrical performance faced by the photovoltaic/thermal energy hybrid system, Ahmed [9] added porous media, DC fans and glass covers to the Photovoltaic/Trombe wall (PV/TW) system. The results show that the use of porous media and DC fans have a positive effect on the system performance, while the glass cover has a negative impact

on system performance. The existence of porous media with DC fans increases the thermal and electrical efficiency of the PV/TW system by 13% and 4%. In addition, the combined effect of porous media, DC fan and glass cover increases the thermal efficiency and electrical efficiency of the system by 20% and 0.5% respectively. Irshad et al. [10–12] used TRNSYS software to provide a simulation model of PV/TW system laboratory and studied the effects of air mass flow rate and three kinds of glass cladding on the performance of PV/TW system. The results show that the addition of argon in PV/TW system can significantly reduce the cooling load and room temperature of the system and increase the photovoltaic output.

Huang et al. [13] conducted a comprehensive study on the thermal performance of a new type of vacuum photovoltaic insulating glass unit (VPV IGU) and the comprehensive optimization design of the photovoltaic enclosure system. A prototype office building model of the photovoltaic curtain wall was constructed through EnergyPlus, and the heat gain, heat loss, heat load, light energy and photovoltaic power generation parameters of different curtain walls were compared. Through comparative analysis, it is proved that VPV IGU has good thermal insulation performance. It can reduce heat gain by 81.63% and 75.03% and heat loss by 31.94% and 32.03% in Hong Kong (HK) and Harbin (HB), respectively. Applying VPV IGU on all available facades of the prototype building can achieve net energy savings of 37.79% and 39.82% under different climatic conditions.

Luo et al. [14] studied the integrated photovoltaic thermoelectric (BIPVTE) wall system in six different cities in China. The results show that the thermal performance of the BIPVTE wall is 10 times that of the ordinary wall, with an additional benefit of 32.7 kWh/m^2 of power generation and 30.91 kWh/m^2 of cooling capacity. The BIPVTE wall system has an energy saving rate of up to 480% compared to conventional wall systems. It is pointed out that further research can be carried out by considering such factors as the air gap between the wall and the photovoltaic panels, the direction of the photovoltaic panels, the wall structure, the airflow and the recovery period.

In summary, the current research of domestic and foreign scholars mainly focuses on the quantitative analysis of the thermal performance of photovoltaic walls and the impact on the indoor environment, while there are relatively few studies on the suitability of different structures (installation) of photovoltaic walls in regions with different climatic conditions. In addition, at present, in the simulation calculation of the thermal performance of various photovoltaic walls, each researcher has adopted a one-dimensional non-heat transfer model, and the calculation and analysis have different emphasis on one side [13, 15–20]. However, due to the shielding of solar radiation by photovoltaic modules and the influence of the air layer left in the middle on heat transfer, the heat transfer process of photovoltaic curtain walls is often more complicated than that of ordinary walls. In this paper, the existing one-dimensional non-large-scale propagation and thermal model is improved by the control volume method. On this basis, the suitability of the photovoltaic wall structure in different regions is studied.

2. Experimental Platform

As shown in Fig. 1, the experimental platform for the research on the thermal performance of the PV wall was built on the south-facing wall of a small house dedicated to experimental research built in real size. The site is located on the roof of a teaching building in Hong Kong Polytechnic University. No other objects obstruct the experimental platform throughout the year.

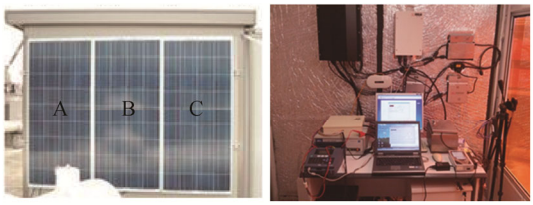

Fig. 1 Physical diagram of the experimental platform

The structures of the three types of PV walls are shown in Fig. 2. Among them, the PV modules in wall A are directly attached to the wall for installation; The B wall is surrounded by 50 mm thick polystyrene boards on the left and right sides of the back of the PV module, so that the upper and lower openings are formed in the middle; C also uses a 50 mm thick polystyrene board to enclose the air layer between the PV module backplane and the wall to prevent it from communicating with the outside world. And the wall thickness is 200 mm.

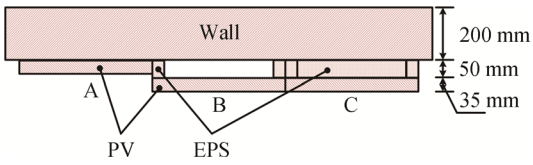

Fig. 2 Schematic diagram of the back structure of the three types of photovoltaic wall (top view)

For the ordinary wall, the measuring points are arranged on the south wall surface of another adjacent experimental cabin with the same enclosure construction method.

Table 1 The main technical parameters of 120 W polysilicon modules used in the experiment

Technical parameter	Numerical value	Technical parameter	Numerical value
Peak power/W	120	Length/mm	1490
Best working point voltage under STC/V	17.2	Width/mm	670
Open circuit voltage under STC/V	21.2	Thickness/mm	35 (Aluminum frame), 10 (module)
Best working current under STC/A	6.86	Quality/kg	10
Short circuit current under STC/A	7.95	Applicable temperature range/°C	–40 to +85

The PV module adopts three 120 W polycrystalline silicon modules, and the relevant technical parameters are shown in Table 1. The inspection instrument is used to inspect the measurement sensor of each parameter, and then the parameters are transferred to the computer for data recording and storage.

The parameters to be tested mainly include the following aspects:

(1) Meteorological parameters

The small weather station is set at 2 m behind the experimental hut, and there is no obstruction from other objects around. The measurement parameters mainly include: outdoor air temperature, humidity, wind direction, wind speed, direct solar horizontal plane and scattered radiation illuminance, and the irradiance on the west vertical plane parallel to the surface of the PV module in this experiment.

(2) Thermal performance parameter test

The temperature measurement points in the PV wall are arranged as shown in Fig. 3. Among them, there are measurement points on the upper, middle and lower back of each PV module; the upper and lower measuring points are respectively $L/10$ (The height of continuous installation of photovoltaic modules in the vertical direction is L) from the upper and lower edges of the PV module, that is about 150 mm, and the middle measuring point is at $L/2$. At the same time, when there is an air layer, the air layer corresponding to the measurement points on the back of the module and the outer surface of the building wall are also arranged with the same number of measurement points.

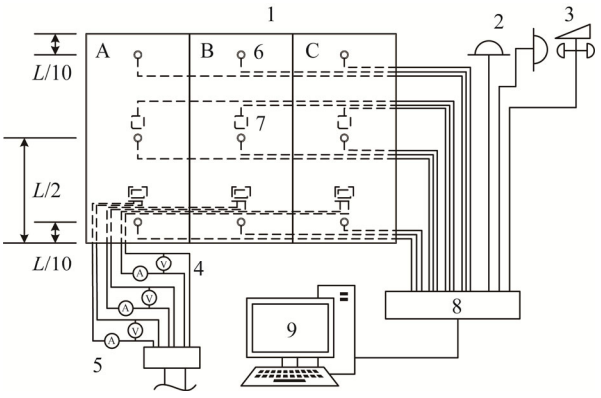

1. Photovoltaic module; 2. Irradiation table; 3. Outdoor wind direction anemometer; 4. Voltmeter; 5. Ammeter; 6. Temperature probe; 7. Heat flow probe; 8. Inspection instrument; 9. Computer

Fig. 3 Data acquisition system diagram of the experimental platform

A heat flow meter is arranged on the inner and outer walls of the wall corresponding to the middle point of each photovoltaic module to record the heat flow of the wall.

(3) Photovoltaic module electrical performance test

For the electrical performance test of the three PV modules, a power test device that can measure the current and voltage in the circuit is installed on the circuit before it is incorporated into the bus box.

3. Mathematical Model

3.1 Photovoltaic wall heat balance heat transfer model

Various PV wall structures involved in this study are shown in Fig. 4(a), (b) and (c). The whole structure is composed of PV modules, building walls and the air layer enclosed between them. According to whether there is an air layer between the photovoltaic module and the building wall, and whether the upper and lower air layers are connected with the outside atmosphere, different mathematical calculation models are established on the overall heat transfer of the PV wall.

In order to simplify the calculation, the following assumptions are made when the calculation model is established:

(1) Since the geometric dimensions of the length and width of PV modules and building walls are much larger than the dimensions of their thickness, the heat conduction problem inside the PV modules and building walls can be regarded as the heat conduction problem inside an infinite plate. At the same time, since the thermal conductivity between the PV module and the materials inside the wall is not studied, it is assumed that the PV module and the wall are homogeneous, and the thermal conductivity between the multi-layer materials and the heat transfer along the x-axis direction are not taken into consideration. Therefore, it is assumed that one-dimensional unsteady heat transfer is inside the two.

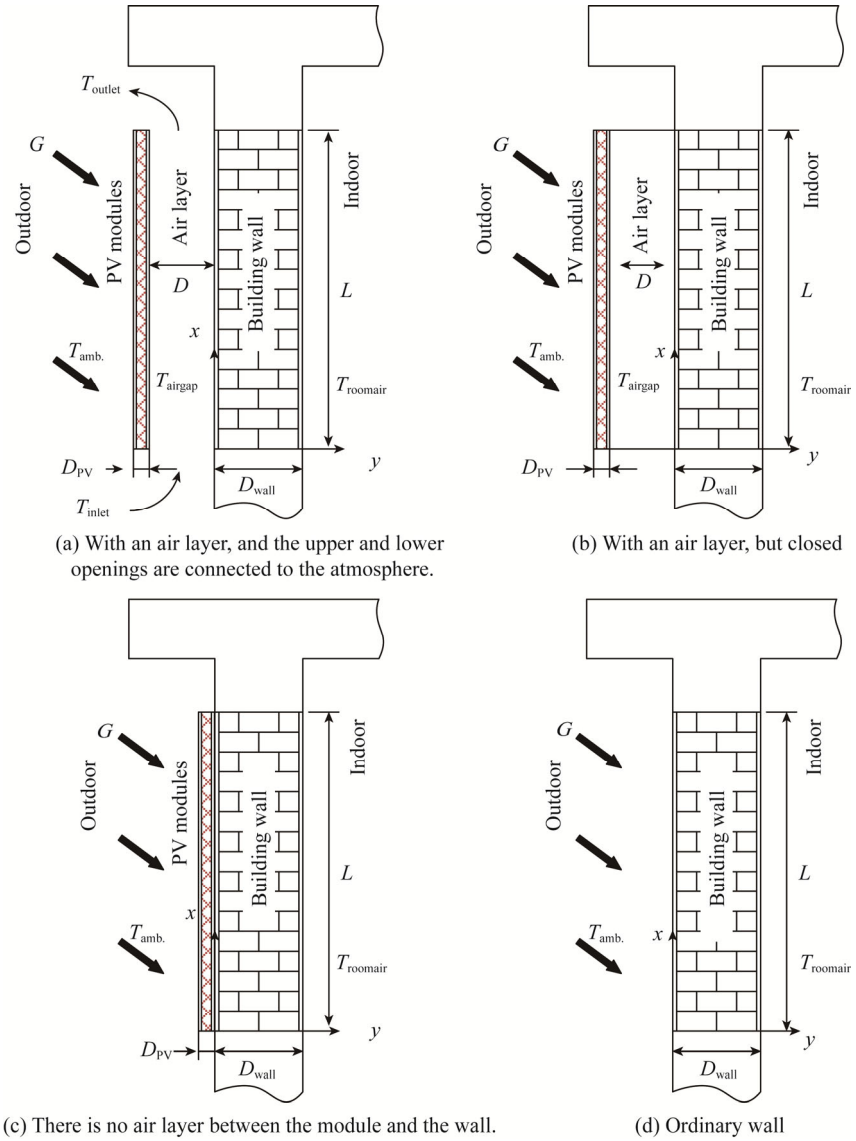

Fig. 4 Schematic diagram of various types of PV walls and ordinary walls

(2) During the calculation process, the physical properties of air, PV modules, walls and other materials remain unchanged;

(3) The velocity component of the flow velocity in the air layer in the y-axis direction is 0, and it is uniformly distributed on the horizontal section of the air layer.

For the PV wall structure with an air layer between the PV module and the wall and the upper and lower openings are connected to the outside air, a two-dimensional coordinate system as shown in Fig. 4(a) is established. The x-axis direction is the air flow direction. The y-axis is perpendicular to the wall surface inward, and the wall corresponding to the lower edge of the PV module is the coordinate origin. The PV wall or ordinary wall of the rest of the structure also uses this coordinate position. The vertical continuous installation height of PV modules is L and the width is W; the thickness of the air layer between the back of the PV module and the outer surface of the building wall is D.

Based on the above assumptions, the thermal balance analysis of the PV wall with upper and lower openings in the air layer is carried out (the rest of the walls can be subtracted from the thermal balance equation of the PV wall with openings in the air layer), which can be divided into the following three parts:

(1) Photovoltaic module

PV modules obtain heat through solar radiation, conduct radiative heat exchange with the external environment and the outer surface of the internal wall, and conduct convective heat exchange with outdoor air and air layer. At the same time, there is a part of electric energy output, and the rest becomes its own internal energy. The temperature changes. Therefore, the corresponding heat balance equation can be expressed as:

$$C_{\mathrm{PV}}M_{\mathrm{PV}}\frac{\partial T_{\mathrm{PV}}}{\partial \tau}=\alpha_{\mathrm{PV}}\left(1-\beta_{\mathrm{PV}}\right)GA-p_{\mathrm{e}}A-h_{\mathrm{PV,out}}A\left(T_{\mathrm{PV,out}}-T_{\mathrm{amb.}}\right)-Q_{\mathrm{PV,out}}-h_{\mathrm{PV,in}}A\left(T_{\mathrm{PV,in}}-T_{\mathrm{airgap}}\right)-\frac{A\sigma\left(T_{\mathrm{PV,in}}^4-T_{\mathrm{wall,out}}^4\right)}{\frac{1}{\varepsilon_{\mathrm{PV,in}}}+\frac{1}{\varepsilon_{\mathrm{wall,out}}}-1} \tag{1}$$

In the above equation,

G is the solar radiation intensity per unit area of the PV module, W/m^2;

A is the PV module area, $A=L\times W$, m^2;

C_{PV} is the specific heat capacity of the PV module, J/(kg·K);

α_{PV} is the absorption rate of the PV module, which is the dimensionless quantity;

β_{PV} is the surface reflectivity of the PV module, which is a dimensionless quantity;

p_{e} is the power output per unit area of the photovoltaic module, W/m^2;

$T_{\mathrm{PV,in}}$ and $T_{\mathrm{PV,out}}$ are the internal and external surface temperature of the PV module, K;

$T_{\mathrm{amb.}}$ is the outdoor air temperature, K;

T_{airgap} is the air layer temperature, K;

σ is the Stefan-Boltzmann constant, $\sigma=5.67\times10^{-8}$ W/(m^2·K^4);

$\varepsilon_{\mathrm{PV,out}}$, $\varepsilon_{\mathrm{PV,in}}$, $\varepsilon_{\mathrm{wall,out}}$ are the emissivity of the outer surface and inner surface of the PV module and the outer surface of the building wall respectively, which are dimensionless quantities;

$h_{\mathrm{PV,in}}$ and $h_{\mathrm{PV,out}}$ are the convective heat transfer coefficients of the inner and outer surfaces of the PV module, W/(m^2·K);

$Q_{\mathrm{PV,out}}$ is the long-wave radiation loss item on the outer surface of the PV module, W.

The PV wall enclosed by the air layer is completely consistent with the above-mentioned circulated form. The heat transfer mechanism of the photovoltaic panel is completely the same, and the heat balance equation of Eq. (1) is adopted; compared with a PV wall with an air layer, the PV wall without an air layer needs to omit the convective heat exchange item between the inner surface and the air layer and the radiation heat exchange item with the outer surface of the wall on the basis of Eq. (1), and increase the heat conduction items between the components and the wall; the ordinary wall has only a single layer of material, which is equivalent to taking the outer surface of the PV module in the PV wall with an air layer as the outer surface of the building wall; the form of heat transfer on the inner surface of the wall remains unchanged, and there is no other form of heat exchange in the middle, only the internal heat conduction of a single material.

(2) Air layer

In the PV wall, the air layer and the PV module backplane and the outer surface of the wall are vertical interlayer heat transfer processes. Therefore, when the ratio of the width D of the air layer to the continuous installation height L of the photovoltaic module, that is $D/L<0.3$, it can be regarded as an infinite space natural convection heat transfer between the middle and vertical plates; when $D/L>0.3$, it can be regarded as natural convection heat transfer between vertical plates in a limited space.

When the air layer communicates with the outside atmosphere, part of the heat from the air flowing through it through convection heat exchange will be taken away by the discharged air, and the remaining heat will be converted into air internal energy, which will increase the temperature of the air layer. The heat balance equation can be expressed as:

$$C_{\mathrm{air}}M_{\mathrm{airgap}}\frac{\partial T_{\mathrm{airgap}}}{\partial \tau}=h_{\mathrm{PV,in}}A\left(T_{\mathrm{PV}}-T_{\mathrm{airgap}}\right)+h_{\mathrm{wall,out}}A\left(T_{\mathrm{wall,out}}-T_{\mathrm{airgap}}\right)-C_{\mathrm{air}}m_{\mathrm{airgap}}\left(T_{\mathrm{outlet}}-T_{\mathrm{inlet}}\right) \tag{2}$$

among them,

T_{inlet} and T_{outlet} are inlet and outlet temperatures of the air layer respectively, K;

$h_{\mathrm{wall,out}}$ is the convective heat transfer coefficient between the air layer and the outer surface of the wall, W/(m^2·K). Since the two walls have similar flow patterns and convective heat transfer rules, $h_{\mathrm{wall,out}}=h_{\mathrm{PV,in}}$;

C_{air} is the specific heat capacity of air, J/(kg·K).

A PV wall with a closed air layer is basically similar to the above-mentioned circulated form in terms of heat transfer mechanism. The difference is: in Eq. (2), because the air layer is closed, there is no last term "$-C_{\mathrm{air}}m_{\mathrm{airgap}}(T_{\mathrm{outlet}}-T_{\mathrm{inlet}})$", that is there is no heat taken away by the outflowing air; the other two types of walls have no air layer, so there is no heat balance equation.

(3) Building wall

The influence on the internal energy of the building wall mainly comes from outdoor solar radiation, convective heat transfer and radiation on both sides of the wall inside and outside, and the corresponding energy balance equation can be expressed as:

$$C_{\mathrm{wall}}M_{\mathrm{wall}}\frac{\partial T_{\mathrm{wall}}}{\partial \tau}=G-h_{\mathrm{wall,out}}A\left(T_{\mathrm{wall,out}}-T_{\mathrm{airgap}}\right)-\sigma A\left(T_{\mathrm{wall,out}}^4-T_{\mathrm{PV,in}}^4\right)\times\left(\frac{1}{\varepsilon_{\mathrm{PV,in}}}+\frac{1}{\varepsilon_{\mathrm{wall,out}}}-1\right)-h_{\mathrm{wall,in}}A\left(T_{\mathrm{wall,in}}-T_{\mathrm{roomair}}\right)-\varepsilon_{\mathrm{wall,in}}\sigma A\left(T_{\mathrm{wall,in}}^4-T_{\mathrm{roomsurface}}^4\right) \tag{3}$$

among them,

T_{roomair} is the indoor temperature, as the initial input parameter, and its value is calculated as the indoor design temperature of heating and air-conditioning in different cities in summer and winter;

$T_{\text{roomsurface}}$ is the surface temperature of other walls and objects in the room, approximately $T_{\text{roomsurface}}=T_{\text{roomair}}$;

$h_{\text{wall,in}}$ is the heat transfer coefficient between the inner surface of the wall and the indoor air, usually $h_{\text{wall,in}}=8.7$ W/(m^2·K);

M_{wall} is the quality of the wall, kg;

C_{wall} is the specific heat capacity of the wall, J/(kg·K);

$\varepsilon_{\text{wall,in}}$ is the emissivity of the inner surface of the wall, which is a dimensionless quantity.

PV walls and ordinary walls with closed air layer and no air layer are completely consistent with the above-mentioned circulated forms, and the boundary conditions and heat transfer mechanism of the wall body surface are completely consistent, therefore Eq. (3) can be used.

3.2 Heating and air-conditioning compound calculation method

3.2.1 Wall heat gain calculation

The heat gain of the wall is still calculated by solving the unsteady heat transfer equation. The Periodic Response Factors (PRF) in the radiation time series method is not directly used. The main consideration is that due to the difference between the structure of the photovoltaic wall with air layer and the conventional wall, the heat transfer of the middle air layer cannot be simply regarded as heat conduction and heat transfer, and it cannot show the influence of the opening of the air layer on the heat gain of the building wall.

For PV walls with an air layer in the middle, according to the conclusions of the above experimental research, the vertical temperature change in the air layer cannot be simply assumed to be linear; if the average temperature is used, it is simply regarded as a one-dimensional heat transfer problem along the axis, and there will be a certain error.

Therefore, in this study, for these two types of photovoltaic walls, based on the above analysis of the thermal balance of each part of the photovoltaic wall, a number of one-dimensional unsteady heat transfer equation solution units are divided into the corresponding wall in the vertical direction, calculating the heat gain of the corresponding wall. Specifically, on the basis of solving the one-dimensional unsteady heat transfer equation of the wall, the corresponding calculation domain is divided into a continuous volume unit in the vertical direction by the control volume method; a corresponding grid is set in each volume unit and the nodes are then solved separately to achieve, as Fig. 5 shows.

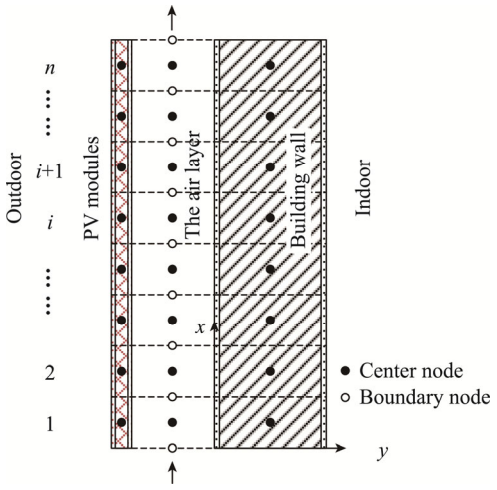

Fig. 5 Schematic diagram of the control unit division in the vertical direction of the photovoltaic wall with an air layer

Therefore, for the air layer with upper and lower openings, according to Eq. (2), the corresponding heat balance equation for each control unit can be expressed as:

$$\begin{aligned} C_{\text{air}}M_{\text{airgap}}\frac{\partial T_{\text{airgap},i}}{\partial \tau} &= h_{\text{PV,in}}A_i\left(T_{\text{PV},i}-T_{\text{airgap},i}\right) \\ &+ h_{\text{wall,out}}A_i\left(T_{\text{wall,out},i}-T_{\text{airgap},i}\right) \\ &- C_{\text{air}}m_{\text{airgap}}\left(T_{\text{outlet},i}-T_{\text{inlet},i}\right) \end{aligned} \quad (4)$$

among them,

$T_{\text{inlet},i}$, $T_{\text{outlet},i}$ respectively represent the inlet and outlet temperature of the control unit, $T_{\text{inlet},i}=T_{\text{outlet},i-1}$;

The first control unit $T_{\text{inlet},1}$ counted from the bottom is approximately equal to the ambient temperature, that is $T_{\text{inlet},1}=T_{\text{amb.}}$, K;

Since the length L_i in the x-axis direction is much smaller than the length D_i in the y-axis direction when the control unit is divided, the temperature of the air in the entire unit is $T_{\text{airgap},i}=(T_{\text{inlet},i}+T_{\text{outlet},i})/2$, K;

A_i is the area in the vertical direction of the unit, $A_i=L_i\times W$, m^2.

Similarly, for the PV modules and building walls in the control unit, according to Eq. (1), the following balance equation also exists:

$$\begin{aligned} C_{\text{PV}}M_{\text{PV}}\frac{\partial T_{\text{PV},i}}{\partial \tau} &= \alpha_{\text{PV}}\left(1-\beta_{\text{PV}}\right)GA_i - p_{\text{e}}A_i \\ &- h_{\text{PV,out}}A_i\left(T_{\text{PV,out},i}-T_{\text{amb.}}\right) \\ &- Q_{\text{PV,out},i} - h_{\text{PV,in}}A_i\left(T_{\text{PV,in},i}-T_{\text{airgap},i}\right) \\ &- \frac{A_i\sigma(T_{\text{PV,in},i}^4-T_{\text{wall,out},i}^4)}{\frac{1}{\varepsilon_{\text{PV,in}}}+\frac{1}{\varepsilon_{\text{wall,out}}}-1} \end{aligned} \quad (5)$$

$$C_{\text{wall}}M_{\text{wall}}\frac{\partial T_{\text{wall},i}}{\partial \tau}=G-h_{\text{wall,out}}A_i\left(T_{\text{wall,out},i}-T_{\text{airgap},i}\right)-\sigma A_i\left(T^4_{\text{wall,out},i}-T^4_{\text{PV,in},i}\right)\times\left(\frac{1}{\varepsilon_{\text{PV,in}}}+\frac{1}{\varepsilon_{\text{wall,out}}}-1\right)-h_{\text{wall,in}}A_i\left(T_{\text{wall,in},i}-T_{\text{roomair}}\right)-\varepsilon_{\text{wall,in}}\sigma A_i\left(T^4_{\text{wall,in},i}-T^4_{\text{roomsurface}}\right) \quad (6)$$

The meaning of each letter is the same as the above equation, and the added subscript i represents the i-th control unit.

According to Eqs. (4)–(6), the corresponding discrete equation can be obtained by numerical solution based on the finite difference method. By solving the discrete equations, and then bringing back the original heat balance equations, the heat transferred into the room is ultimately the sum of the convective heat exchange between the inner surface of the building wall and the indoor air and the radiative heat exchange between the surface of other objects in the room.

3.2.2 Load calculation method and radiation time coefficient

(1) Load calculation method

For load, the main difference from heat gain lies in the radiation heat exchange part of heat gain. The heat entering the room through the convection heat exchange between the inner surface of the wall and the indoor air becomes an instantaneous load immediately; the part of the radiant heat exchange between the inner surface of the wall and other objects is stored in the indoor objects, which makes the surface temperature of the object change, and then passes through the convection heat exchange with the air for a certain period of time, and finally enters the room to form a load.

In this study, the Radiant Time Factors (RTF) in the radiant time series method is used to simplify the calculation for calculating the room load from the heat gain.

In the weighting coefficient method, the cooling load Q_θ at time θ can be expressed as the relationship between the instantaneous heat gain (q_θ, $q_{\theta\text{-}n\Delta\tau}$) at the current moment and the previous moment, the cooling load at the previous moment ($Q_{\theta\text{-}\Delta\tau}$, $Q_{\theta\text{-}2\Delta\tau}$,... $Q_{\theta\text{-}n\Delta\tau}$) and the heat gain weight coefficient (v_0, v_1, …, v_n, w_1, w_2, …, w_n).

$$Q_\theta=v_0q_\theta+v_1q_{\theta-\Delta\tau}+\cdots+v_nq_{\theta-n\Delta\tau}-w_1Q_{\theta-\Delta\tau}-w_2Q_{\theta-2\Delta\tau}-\cdots-w_nQ_{\theta-n\Delta\tau} \quad (7)$$

For the radiation time series method, it is further simplified. When calculating the load from the heat gain, the radiation time coefficient of 24 hours a day (item) is used, and the radiation part of the heat gain is directly converted into the cooling load without complicated conversion calculations, as shown in the following equation:

$$Q_\theta=r_0q_\theta+r_1q_{\theta-\Delta\tau}+r_2q_{\theta-2\Delta\tau}\cdots+r_{23}q_{\theta-23\Delta\tau} \quad (8)$$

Among them, r_0, r_1, r_2, ..., r_{23} are the radiation time coefficients, and the sum is 1. Its value is closely related to the thermophysical properties, number of surfaces and angles of the objects in the room, indicating the proportion of the radiant heat that will be released from time to time to form a load in the next 24 hours.

(2) Wall structure and material property parameters

For this study, the indoor space of the building was calculated with reference to the actual geometric dimensions of the experimental house; the thermal performance of the envelope structure is selected to determine the relevant parameters for the three regions of Hong Kong, Changsha and Beijing. The building walls of the three regions selected in the calculation are divided into exterior layer, middle layer and interior layer. Table 2

Table 2 Thermal performance parameters of various materials involved in the calculation

	Material name	Thermal conductivity λ/W·m^{-1}·K^{-1}	Density ρ/ kg·m^{-3}	Specific heat capacity C/J·kg^{-1}·K^{-1}	Thickness d/ mm
PV module [21]	Multilayer material	0.5868	1444	1229	10
Aluminum edging	Aluminum profile	237	2719	871	2
Experimental hut wall/ Hong Kong ordinary wall	Cement mortar δ_1	0.72	1860	1050	10
	Concrete δ_2	1.73	2400	840	150
	Interior layer δ_3	0.38	1120	840	10
Changsha ordinary wall	Cement mortar δ_1	0.93	1800	1050	10
	Concrete δ_2	0.58	1400	1062.3	240
	Interior layer δ_3	0.81	1600	1050	10
Beijing ordinary wall	Cement mortar δ_1	0.93	1800	1050	10
	Concrete δ_2	0.2	500	1461.4	300
	Interior layer δ_3	0.81	1600	1050	10

shows the structure of photovoltaic modules and corresponding building walls and the physical parameters of each layer of material. Table 3 shows the optical parameters of each surface.

Table 3 Optical performance parameters of each surface

Parameter	The values
Absorption rate of the outer surface of the PV module α_{PV}	0.90
Absorption rate of the outer surface of the wall $\alpha_{wall,out}$	0.90
Reflectivity of the outer surface of the PV module β_{PV}	0.04
The outer surface emissivity of photovoltaic modules $\varepsilon_{PV,out}$	0.90
PV module back emissivity $\varepsilon_{PV,in}$	0.89
The outer surface emissivity of the wall $\varepsilon_{wall,out}$	0.50
Surface emission coefficient of aluminum cladding ε_{Al}	0.29

(3) Radiation time coefficient calculation

According to the above parameters and the RTF calculation method provided in Ref. [22], other objects or surfaces in the experimental cabin are not considered, and are only enclosed by the six surfaces of the enclosure structure. From this, the RTF values of the experimental huts formed by the corresponding building walls in the three cities of Hong Kong, Changsha and Beijing were calculated, as shown in Fig. 6. According to the thermophysical properties of the three urban wall materials and the thickness of each layer, the RTF value decays with time showing different trends as shown in the figure.

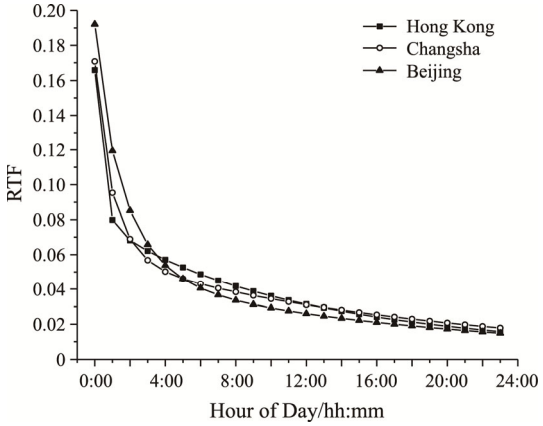

Fig. 6 Calculated RTF values of experimental huts formed by corresponding building walls in three cities

3.3 Verification of accuracy of calculation results

In this study, Matlab software was used to program the heat transfer and formed load of the above-mentioned various PV walls and ordinary walls. In order to verify the accuracy of the above-mentioned numerical calculation model, the calculation results are compared with the experimental results, and the root mean square index is used to evaluate the differences between the two:

Root mean square error (RMSE):

$$\mathrm{RMSE} = \sqrt{\frac{1}{n}\sum_{i=1}^{n}\left(C_i - E_i\right)^2} \tag{9}$$

Among them, C_i is the calculated value and E_i is the experimental value.

In addition, RMSE indicates the degree of dispersion between the calculated value and the experimental value. The smaller the corresponding value, the closer the calculated value of the model is to the measured value.

The following is a comparison of the temperature calculation results and experimental test values of various PV walls and ordinary walls:

(1) Photovoltaic wall with upper and lower openings in the air layer

As shown in Fig. 7, according to the above evaluation indicators, the error between the calculated value of the backplane temperature of the PV module and the temperature of the open air layer and the experimental value is relatively large, which mainly occurs at the inflection point.

(2) PV wall with closed air layer

As shown in Fig. 8, the difference between the calculated and experimental values of the surface temperature of the PV wall with closed air layer is slightly smaller than that of the PV wall with open air layer. The temperature error of the PV module backplane is mainly from night to morning sunrise and afternoon.

(3) PV wall without air layer

As shown in Fig. 9, the agreement between the calculation results of the surface temperature of the PV wall without an air layer and the experimental results is significantly higher than that of the PV wall enclosed by the air layer.

(4) Ordinary wall

As shown in Fig. 10, the calculation results of the internal and external surface temperature of the ordinary wall are in good agreement with the experimental results. Obvious errors also appear at the inflection point of the minimum and maximum temperature.

For the calculation results and experimental results of the above-mentioned various walls, relatively large errors appear in the morning at sunrise and in the afternoon. The analysis is due to the corresponding simplifications in the calculation, and there is no distinction between direct and scattering in solar radiation. When the solar radiation intensity is significantly reduced in the morning at sunrise and in the afternoon, the composition ratio of direct and scattered radiation changes greatly. The spectral composition of direct and scattered radiation is

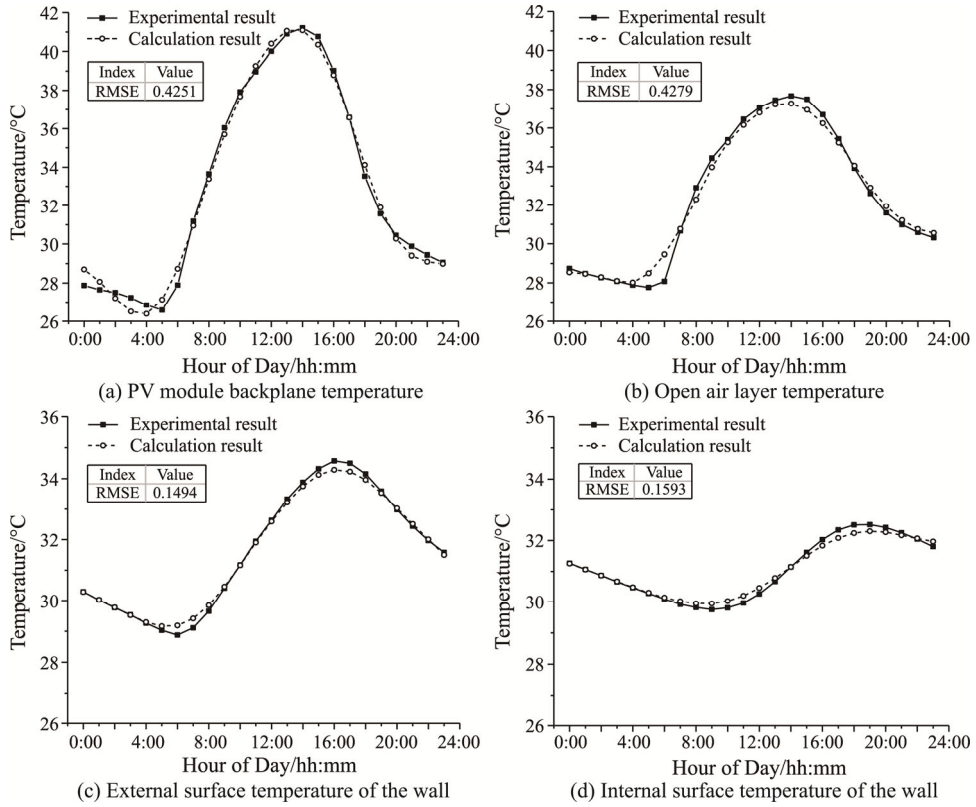

Fig. 7 Comparison of calculation and experimental results of each surface temperature of the photovoltaic wall with the upper and lower openings of the air layer

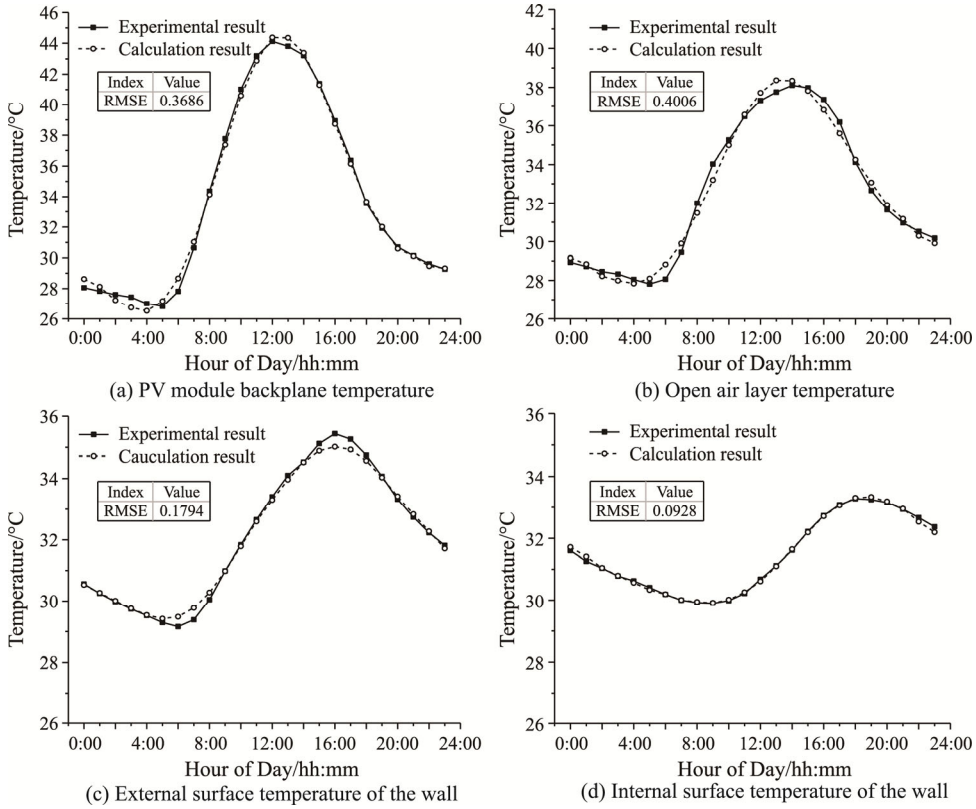

Fig. 8 Comparison of the calculated and experimental results of the surface temperature of the photovoltaic wall enclosed by the air layer

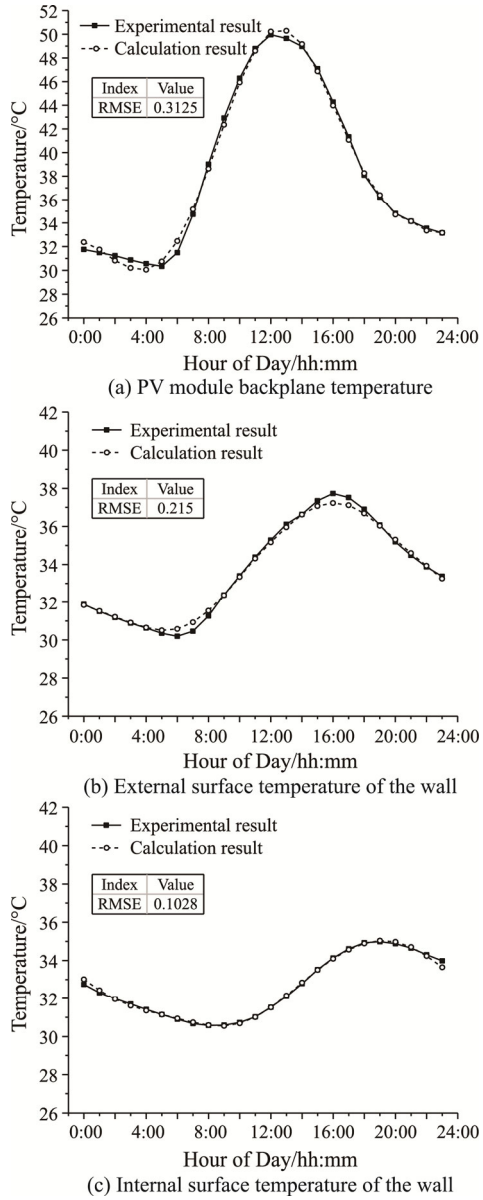

Fig. 9 Comparison of calculation and experimental results of surface temperature of photovoltaic wall without air layer

different, so the photovoltaic module or wall absorbs different solar radiation heat at different moments. Therefore, a relatively large error is generated for the temperature of the back panel of the photovoltaic module. After transmission, the same error occurs in the air layer and the outer surface of the wall.

By comparing the temperature calculation results of all parts of the above four walls with the experimental results, it can be seen that they are in good agreement. Therefore, it can be considered that the theoretical calculation model and solution method established above are relatively accurate for the calculation results of all kinds of PV walls and ordinary walls.

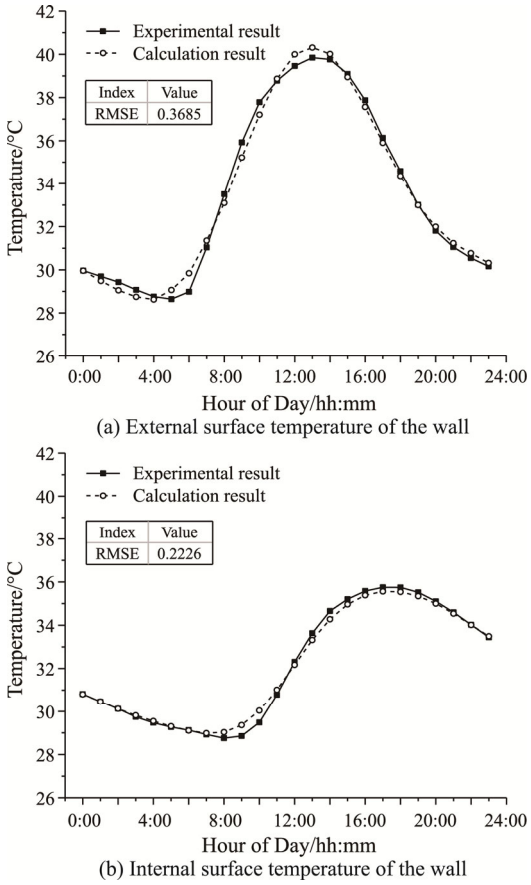

Fig. 10 Comparison of calculation and experimental results of internal and external surface temperature of ordinary walls

4. Suitability Analysis of Various Types of PV Walls

China's relevant regulations [23] divide China into seven major climate zones based on the principle of combining comprehensive analysis and leading factors. Among them, most of Beijing (116.28° E, 39.93° N) is in a cold area and belongs to the II building climate zone. The basic requirements for buildings in this area should meet the requirements of cold protection, heat preservation, and frost protection in winter, and heat protection in some areas in summer; Changsha (112.92° E, 28.22° N) is located in an area with hot summer and cold winter, and belongs to the III architectural climate zone. The buildings in this area should meet the requirements of heat prevention, ventilation and cooling in summer, and adequate protection from cold in winter; Hong Kong (115.12° E, 21.23° N) is located in an area with hot summer and warm winter, and belongs to the IV architectural climate zone. This area should fully meet the requirements of heat protection, ventilation and rain protection in summer, and cold protection and heat preservation are not

considered in winter. Considering that the selected three cities have typical differences in the building envelope structure, photovoltaic walls with different construction methods may have different effects on indoor heat gain or heat loss and heating and air conditioning loads, so the above three are selected in the calculation. The urban summer and winter typical day weather parameters are used as input for calculation and comparative analysis.

Fig. 11 shows the curves of solar irradiance and outdoor ambient temperature of the three cities on typical days in summer and winter in different orientations. Among them, the irradiance on the east (–90°, 0°), south (0°, 0°) and west (90°, 0°) surfaces of each city is calculated from the corresponding values of the typical year meteorological parameters [24] on the horizontal plane (0°, 90°) and the longitude and latitude of each city.

According to the summer and winter weather parameters of different cities and the thermal performance of the building envelope, the calculation models established above are used to calculate the photovoltaic walls and ordinary walls of different structural forms; the heat gain in summer and the heat loss in winter are obtained for various types of walls indoors, and then the heat and cold loads generated are calculated. The specific results and corresponding comparative analysis are as follows.

4.1 Heat gain and cooling load in the summer

The three cities use walls with different structures in different orientations to gain indoor heat in summer as shown in Fig. 12. By comparing all kinds of walls, it can be seen from Fig. 12 that from around noon to midnight,

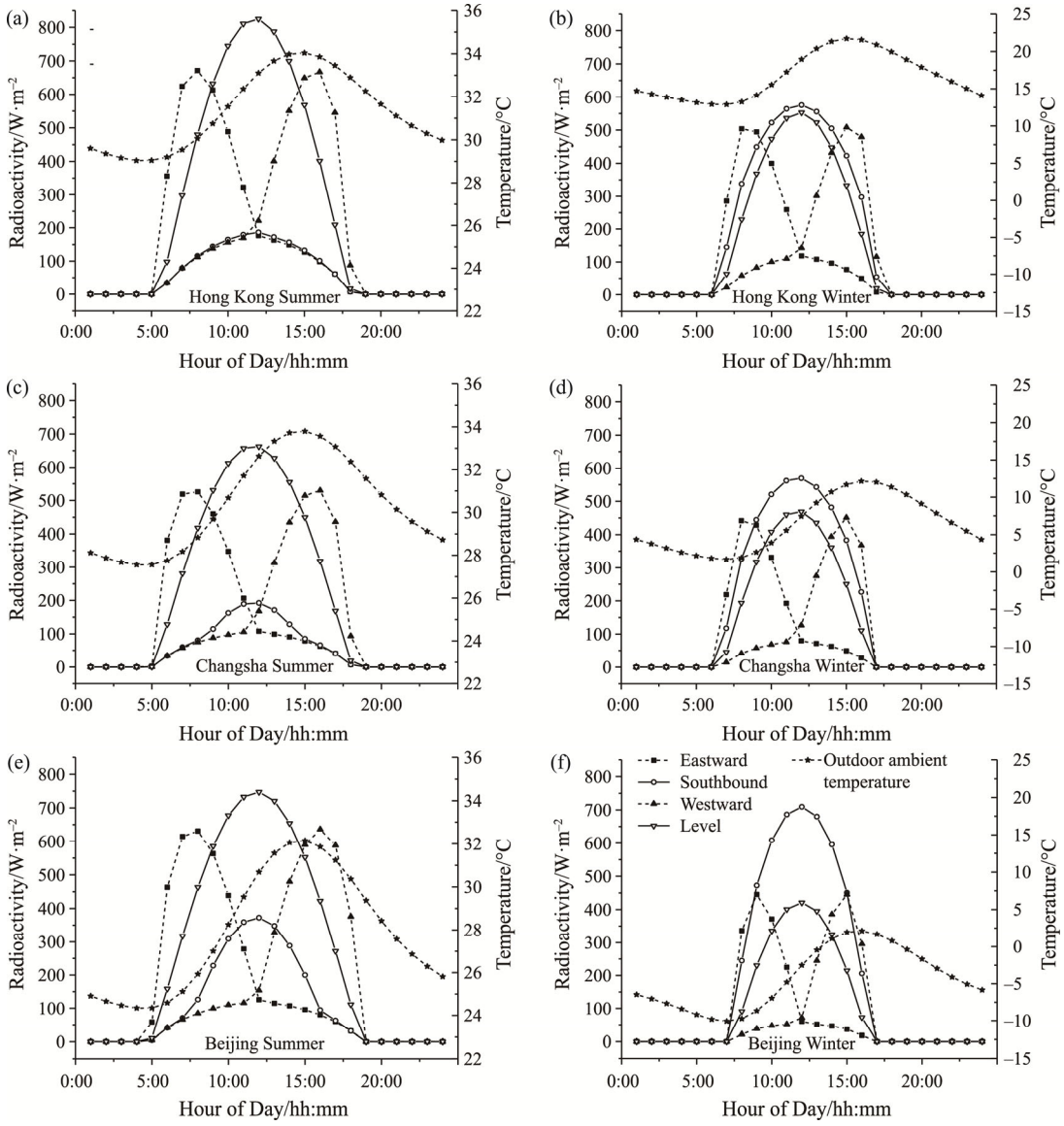

Fig. 11 The outdoor meteorological parameters of the three cities used as input items in the calculation

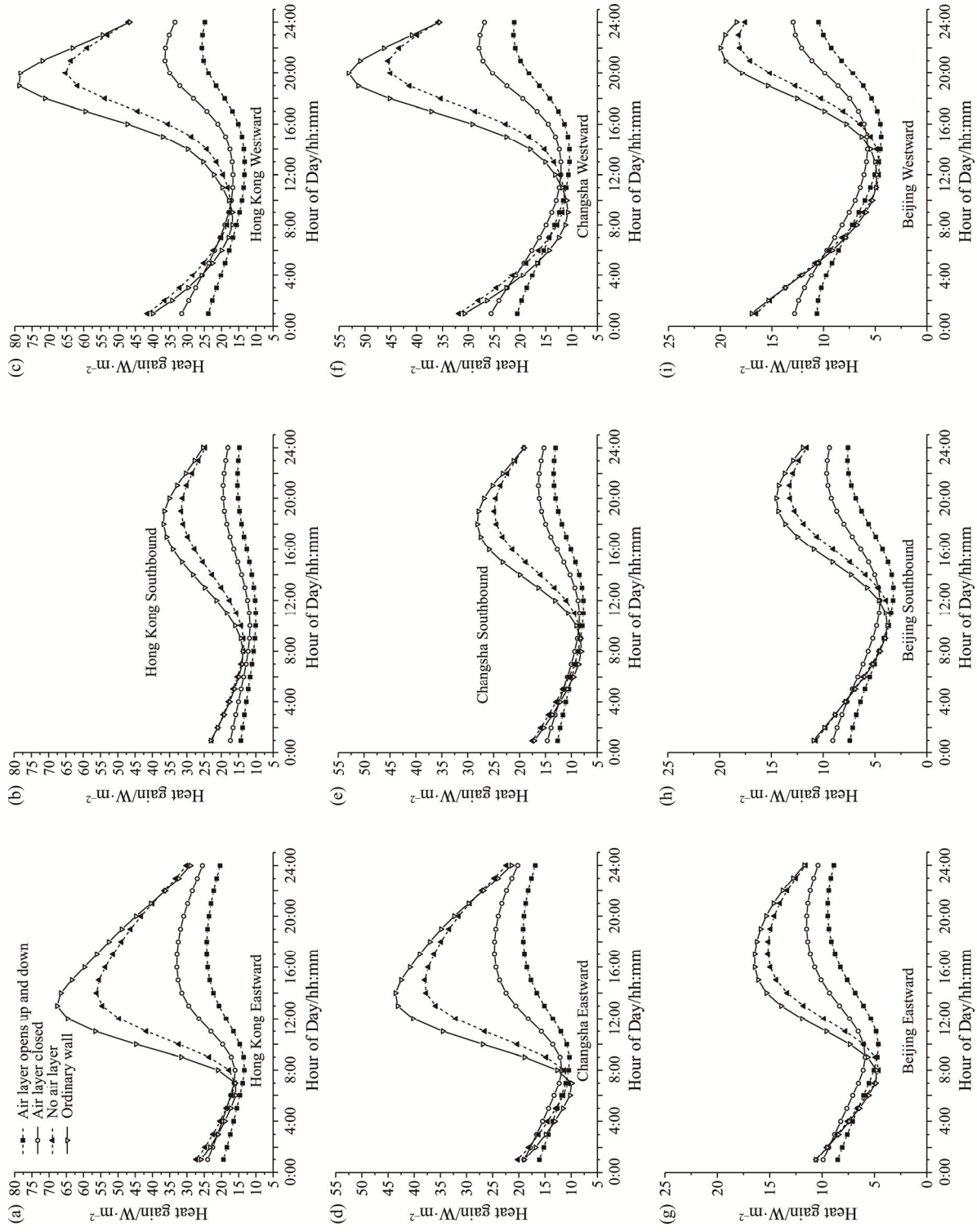

Fig. 12 Comparison of calculation results of indoor heat gain caused by various types of walls in different situations

for different cities and different orientations, the three kinds of photovoltaic walls can reduce the indoor heat gain to a certain extent, reduce the fluctuation range of the heat gain throughout the day, and at the same time make the peak value of heat shift back. The PV wall with air layer opening is the most obvious, and its peak value of indoor heat is only 32.6%–57.6% of that of ordinary wall, with a maximum decrease of about 36 W/m^2 compared with ordinary wall. Meanwhile, the fluctuation range of all-day heat is only about 5–10 W/m^2; the second is the PV wall closed with air layer, but compared with the ordinary wall, the reduction of heat gain is also more obvious; the PV wall without air layer makes the indoor heat only slightly lower than the ordinary wall, and its role is more limited in the south with smaller irradiance or the thermal performance of the wall itself is better in Beijing.

After midnight, especially in the early morning or part of the morning, in Changsha and Beijing, two types of walls with upper and lower air layers and closed air layers appeared, which made indoor heat gain higher than ordinary walls, especially PV walls with closed air layers. The maximum increment can be about 2 W/m^2. It can be seen that the increased air layer and PV modules affect the heat dissipation of the wall at night to a certain extent.

According to the above heat gain, the cooling load generated by each wall to the room is calculated, as shown in Fig. 13. Comparison of all kinds of walls, the three kinds of PV walls can reduce the indoor air conditioning load to a certain extent, so that the fluctuation range of cold load formed by the wall throughout the day is reduced, but the effect of the PV wall with the air layer opening is more obvious. In various cases, the peak value of the formation of cooling load is 37.5%–62.6% of the peak value of the ordinary wall, and the maximum can be reduced by 37 W/m^2 (Hong Kong westward); for the closed PV wall cooling load of the air layer, it is slightly higher than the open one. In Hong Kong and Changsha, the cooling load is significantly lower than that of the ordinary wall throughout the day, but in Beijing, the cooling load is slightly higher than that of the ordinary wall in all directions from morning to noon. The cooling load of the wall without air layer is close to that of the ordinary wall.

By comparing all kinds of walls with different orientations, according to the ratio of peak cooling load, the western-facing photovoltaic wall with various forms reduces the room cooling load more obviously, and the ratio of peak cooling load to ordinary wall is 37.5%–95%, followed by 41.3%–96.1% in the eastward direction, and 45.6%–95.6% in the south direction.

Compared with different cities, Hong Kong adopts various forms of PV walls in all directions, and the reduction of cooling load is the most obvious, followed by Changsha and finally Beijing. Only when the PV walls closed by air layer are used in Beijing, the cooling load of some PV walls is slightly higher than that of ordinary walls and PV walls without air layer.

4.2 Heat loss and heat load in winter

In winter, the three cities adopt different structures of walls in different orientations, so that the heat loss generated indoors is shown in Fig. 14. In part of the time period before 14:00, the PV wall closed with air layer can effectively reduce the indoor heat loss for different cities and different orientations, and its peak value is only 14.5%–84.6% compared with the ordinary wall. Among all kinds of PV walls, the reduction effect is the most obvious, with the maximum reduction up to 19.7 W/m^2 (Changsha southward); however, after 14:00, the heat loss of the southward common wall in some cities is lower than that of the PV wall closed by air layer. The heat loss of the PV wall with the upper and lower openings of the air layer is higher than that of the PV wall with the closed air layer (except for the period when the heat loss is negative in Hong Kong), and the difference between the two is 0.5–8.2 W/m^2; however, compared with ordinary walls, the heat loss value and peak value are lower than ordinary walls most of the time; but in some periods after 14:00, the heat loss value is significantly greater than that of other types of walls, especially in Beijing. The heat loss of the PV wall without an air layer is reduced to a certain extent compared with the ordinary wall in the part of the period before 14:00, and then it is not obvious. It can be seen that the solar radiation shielding by PV modules during the day, the existence of the air layer and the influence of the opening on the heat gain of the wall increase the heat loss in disguised form.

According to the above-mentioned different wall heat losses in each city, the heat load to the indoor can be calculated accordingly, as shown in Fig. 15. The thermal load of PV wall closed with air layer is the lowest in different orientations in different cities. Compared with the ordinary wall, its peak value is only 42.9%–85.4% of that of the ordinary wall, and the maximum value can be reduced by 16.7 W/m^2 (Changsha southward). The thermal load of PV walls with air openings above and below the air layer is always greater than that of those with air layer closed, and the difference between them remains at 2.1–7.4 W/m^2. Meanwhile, the thermal load of PV walls with air layer openings in Changsha is still smaller than that of ordinary walls and PV walls without air layer throughout the day. However, in Hong Kong and Beijing, the thermal load of photovoltaic walls with air layer openings is always higher than that of PV walls with air layer closed. The thermal load of the open PV wall in the air layer is obviously higher than that of the

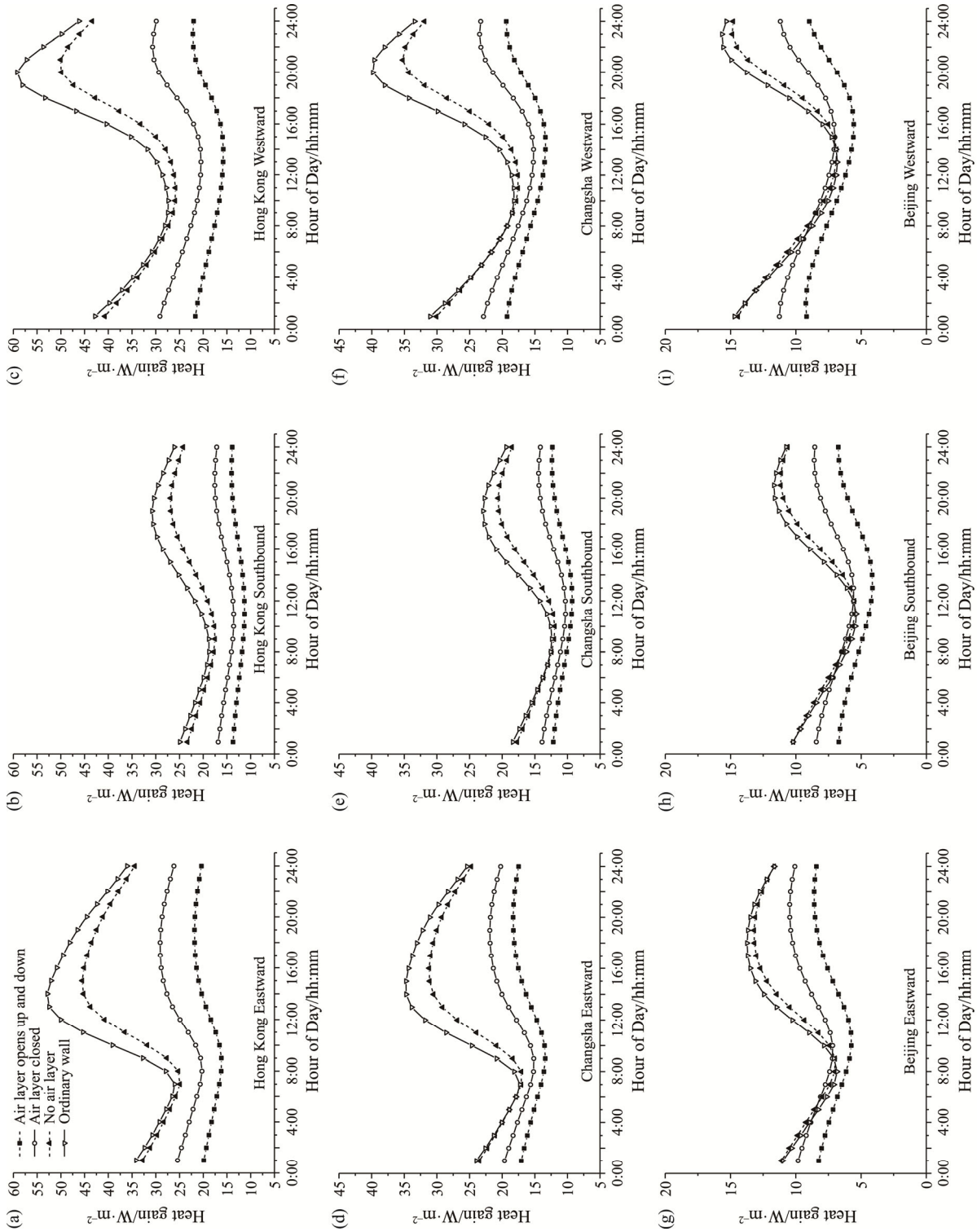

Fig. 13 Comparison of calculation results of indoor cooling load caused by various walls under different conditions

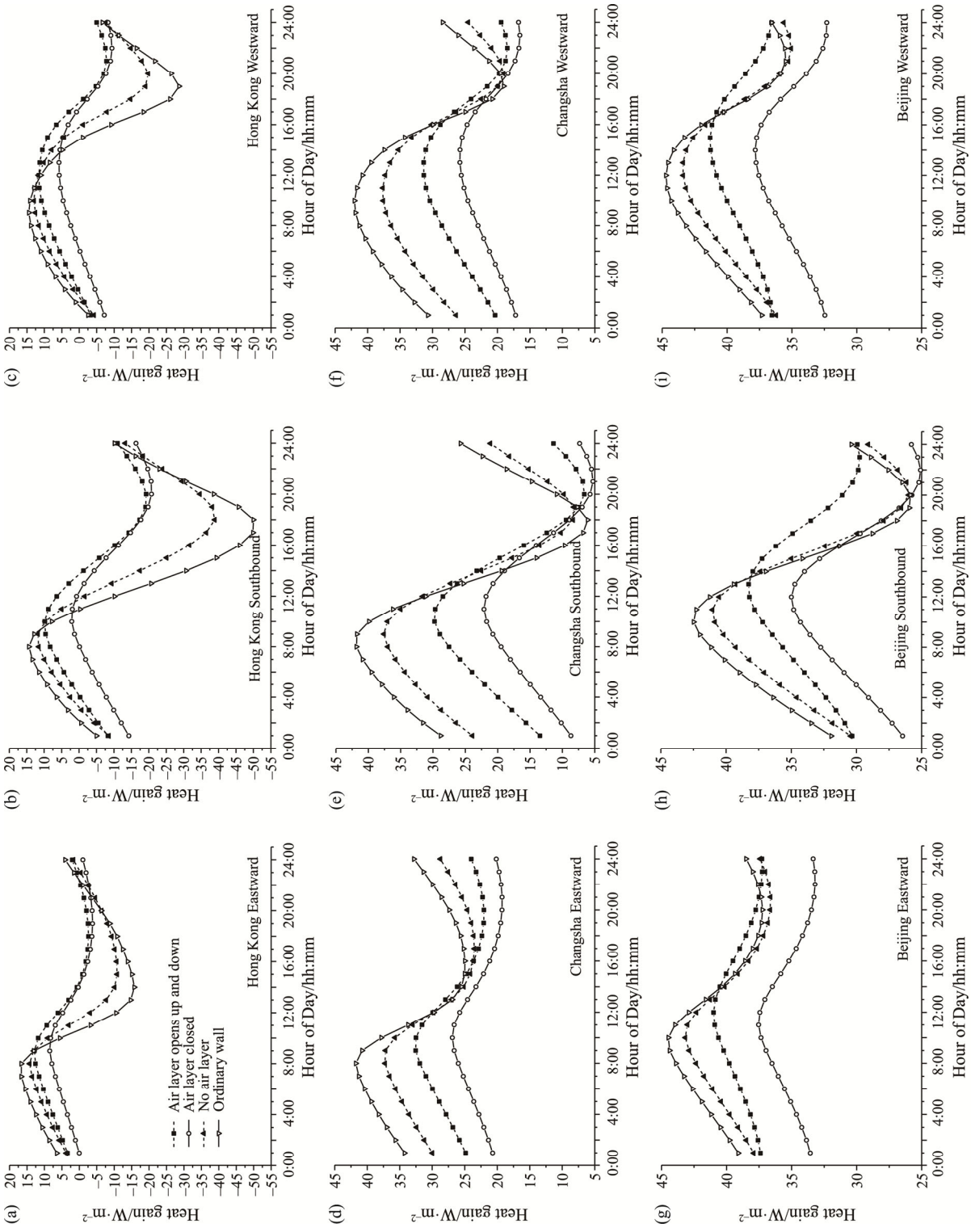

Fig. 14 Comparison of calculation results of indoor heat loss caused by various types of walls in dif-ferent situations

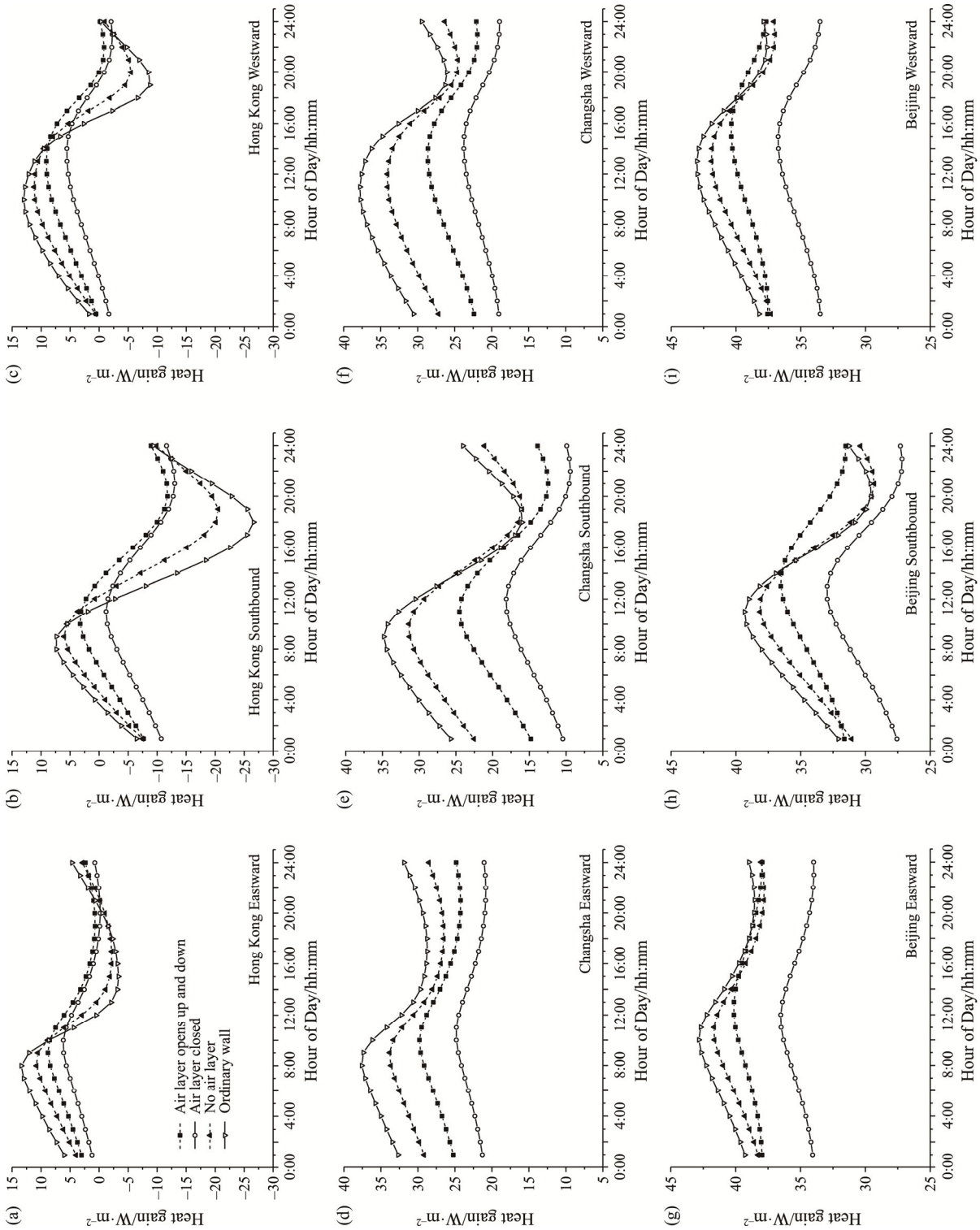

Fig. 15 Comparison of the calculation results of the heat load formed by various walls on the room un-der different conditions

ordinary wall. For the photovoltaic wall without air layer, it is slightly lower than the ordinary wall on the whole, but it is slightly higher than the ordinary wall in the south of some cities around 14:00–20:00.

Comparing various types of walls with different orientations, the application of various PV walls in the south direction in winter will reduce the heat load more significantly. The ratio of the peak heat load of the southward PV walls to the ordinary walls are 44.3%–97.0%, followed by eastward is 46.0%–97.3%, and then westward is 42.9%–97.4%.

Comparing different cities, it can be clearly seen that the reduction (percentage) of the heat load of various types of PV walls in Hong Kong is higher than that of the other two cities; while in Changsha, the reduction in heat load is more obvious.

4.3 Suitability analysis of different cities

(1) Under ideal conditions

According to the comparison and analysis of the above various types of PV walls in summer heat gain, winter heat loss and cooling and heating load in different cities in different directions with ordinary walls, the most ideal choice for various types of PV walls is: in summer, the use of PV walls with upper and lower openings in the air layer and connected to the outside atmosphere is the most effective for reducing indoor heat gain and cooling load; in winter, the use of a PV wall enclosed by an air layer is the most effective for reducing indoor heat loss and reducing indoor heat load.

(2) In the middle conditions

In actual engineering, some active or passive ways can be adopted to make the air layer in the PV wall open or close according to different seasons, so as to realize the above-mentioned ideal operation mode, but at the same time, it is bound to increase the complexity of the wall structure and the existence of reliability problems. Therefore, according to the calculation results of various types of PV walls in different directions in each city, a certain compromise can be adopted to choose whether to open or close in response to the decline in the cooling and heating load throughout the year.

For the various PV walls in different directions in the three cities, a comprehensive comparison is made here based on the sum $\Delta Q_{i,\text{total}}$ of the reduction amplitudes $\Delta Q_{i,\text{cooling}}$ and $\Delta Q_{i,\text{heating}}$ of their peak cold and heat loads relative to the ordinary wall, and the maximum value $\Delta Q_{\max}$ is taken as the optimal:

$$\Delta Q_{\max}=\text{Max}\left(\Delta Q_{\text{vent,total}},\Delta Q_{\text{no vent,total}},\Delta Q_{\text{no gap,total}}\right) \quad (10)$$

$$\Delta Q_{i,\text{total}}=\Delta Q_{i,\text{cooling}}+\Delta Q_{i,\text{heating}}, \quad i=\text{vent, no vent or no gap} \quad (11)$$

among them:

$$\Delta Q_{i,\text{cooling}}=Q_{\text{normal,cooling,max}}-Q_{i,\text{cooling,max}} \quad (12)$$

$$\Delta Q_{i,\text{heating}}=Q_{\text{normal,heating,max}}-Q_{i,\text{heating,max}} \quad (13)$$

The corresponding calculation results are shown in Table 4.

Table 4 The sum of the difference between the peak cold and heat load of different PV walls and the ordinary wall

		Air layer opening	Air layer closed	No air layer
Eastward	Hong Kong/W·m^{-2}	**35.6**	31.0	9.9
	Changsha/W·m^{-2}	24.2	**25.6**	7.3
	Beijing/W·m^{-2}	7.8	**9.6**	1.7
Southbound	Hong Kong/W·m^{-2}	**20.8**	20.6	5.2
	Changsha/W·m^{-2}	20.8	**25.2**	5.7
	Beijing/W·m^{-2}	7.7	**9.5**	1.7
Westward	Hong Kong/W·m^{-2}	**40.9**	36.0	10.9
	Changsha/W·m^{-2}	29.6	**30.4**	8.3
	Beijing/W·m^{-2}	9.1	**10.7**	1.9

Note: The black body in the table refers to the case where the sum of the cold and heat load peaks relative to the reduction range of the ordinary wall achieves the maximum value among the three types of photovoltaic walls.

For Hong Kong, according to Table 4, in the east, south, and west directions of the PV wall with openings in the air layer, the sum of the peak reduction of cold and heat load is greater than that of the PV wall with closed air layer or the PV wall without air layer. Therefore, for low-latitude areas in the south, such as Hong Kong, where outdoor temperature and solar radiation levels are relatively high, PV walls with open air layers can be used throughout the year for ventilation and heat dissipation. When the air layer is closed in the south direction, the reduction of the peak cold and heat load relative to the ordinary wall is only slightly smaller than when the air layer is open, which means that this type of PV wall can also be used. The analysis is mainly because the southward solar irradiance in Hong Kong in summer is relatively small; the heat dissipation requirement after sun exposure is relatively small, and the indoor heat load in Hong Kong is also relatively small in winter, so this method can also be used in the south for the purpose of heat insulation.

For Changsha, according to Table 4, when a PV wall enclosed by an air layer is used in the south, the sum of the reduction of the peak cold and heat load is significantly greater than that of the two PV walls with open air layer and no air layer. It can be seen that due to the low solar irradiance in Changsha in summer, the demand for heat dissipation is relatively small; in winter, due to the climatic characteristics, the outdoor temperature is relatively low, and the lightweight

envelope structure itself has a relatively large demand for heat preservation. Therefore, the air layer can be closed throughout the year, which tends to meet the purpose of heat preservation and heat insulation. For the photovoltaic wall with closed air layer in the east and west, the sum of the corresponding cold and heat load peak reductions is the largest compared to the other two PV walls, but there is no obvious advantage compared with the PV wall with open air layer, especially in the west. For the purpose of heat preservation and heat insulation, a closed air layer can be used throughout the year; while for ventilation and heat dissipation, an open air layer can be used. Therefore, for areas similar to Changsha, the south direction can be biased towards the purpose of thermal insulation in winter, using PV walls enclosed by air layers; the east and west directions can be biased towards the summer for the purpose of ventilation and heat dissipation, using a PV wall with an open air layer, or biased towards the use of a PV wall closed by the air layer in winter.

For Beijing, the use of various photovoltaic walls to reduce the cooling and heating load is not as obvious as the other two cities, but it still has a certain effect. It can be seen from Table 4 that in the east, south and west directions of the PV wall enclosed by the air layer, the sum of the peak cold and heat load reduction relative to the ordinary wall is significantly greater than that of the other two PV walls. Therefore, similar to the northern area of Beijing, it can focus on the purpose of thermal insulation in winter, and adopt a PV wall enclosed by an air layer.

5. Conclusions

In this paper, a simulation study on the heat transfer performance of PV walls with three structural forms of air layer opening, air layer closed and no air layer is carried out, and the accuracy of the simulation is verified by comparison with the design experimental data. The main conclusions are as follows:

(1) The calculation method of the existing one-dimensional unsteady heat transfer model is improved. The corresponding calculation domain is divided into multiple continuous volume elements in the vertical direction through the control volume method, and the grid nodes are solved separately. It has realized the simulation calculation of the temperature and heat flow of each part in the four structural forms of the three PV walls and the ordinary wall of air layer opening, air layer closed and no air layer, and combined with the experimental data, the accuracy of the calculation model improved by this method is verified by using the RMSE as the evaluation basis. The comparison results show that the calculated results are in good agreement with the experimental results, and the calculation results of the theoretical calculation model have high accuracy.

(2) There are certain differences in climate types and building envelopes in different regions. Indoor heat gain or heat loss and heating and air conditioning loads in different regions are different. Through the comparison of simulation data in different cities, it is found that PV walls with different construction methods will also have different effects on indoor heat gain or heat loss and heating and air conditioning loads.

(3) Based on the meteorological data of three typical cities located in different climatic regions and the sum of the difference between the peak cooling and heating loads of different photovoltaic walls in different cities and ordinary walls, the suitability of different PV walls in different regions is summarized. When choosing the form of PV wall, for the southern region, the ventilation and heat dissipation in summer should be emphasized, and the form of PV wall with openings in the air layer communicating with the outside atmosphere should be adopted; for the northern regions, the heat preservation and heat insulation in winter should be emphasized, and the PV wall with closed air layer should be adopted; for the middle hot summer and cold winter area or transition area, the purpose of ventilation and heat dissipation or thermal insulation should be considered according to the solar radiation on the wall surface in winter and summer, the outdoor environment temperature and the thermal performance of the building wall itself, so as to determine whether the air layer in the middle of the PV wall is open or closed.

Acknowledgements

This study was supported by the National Natural Science Foundation of China (Grant No. 51908287) and the Opening Funds of State Key Laboratory of Building Safety and Built Environment and National Engineering Research Center of Building Technology (Grant No. BSBE2020-7).

References

[1] Li G., Zhao X., Ji J., Conceptual development of a novel photovoltaic-thermoelectric system and preliminary economic analysis. Energy Conversion and Management, 2016, 126: 935–943.

[2] Chen H.F., Ji J., Pei G., et al., Experimental and numerical comparative investigation on a concentrating photovoltaic system. Journal of Cleaner Production, 2018, 174: 1288–1298.

[3] Chen H., Li G., Y Jie., et al., Experimental and comparison study on two solar dish systems with a high concentration ratio. Journal of Thermal Science, 2019, 28:

1205–1211.

[4] Zhang C., Chao S., Shen W., et al., A review on recent development of cooling technologies for photovoltaic modules. Journal of Thermal Science, 2020, 29: 1410–1430.

[5] Liu Z.B., Li A., et al., Performance study of a quasi grid-connected photovoltaic powered DC air conditioner in a hot summer zone. Applied Thermal Engineering Design Processes Equipment Economics, 2017, 121: 1102–1110.

[6] Zhang X., Li M., Ge Y., et al., Techno-economic feasibility analysis of solar photovoltaic power generation for buildings. Applied Thermal Engineering, 2016, 108: 1362–1371.

[7] Gao F., Chen J., Lin W., Experimental study on heat dissipation performance of photovoltaic wall with ventilation channel. Building Energy Saving, 2019, 47(4): 17–20.

[8] Luo Y.Q., Zhang L., Liu Z., et al., Performance analysis of a self-adaptive building integrated photovoltaic thermoelectric wall system in hot summer and cold winter zone of China. Energy, 2017, 140: 584–600.

[9] Omer K. Ahmed, Hamada K.I, Salih A.M., Enhancement of the performance of Photovoltaic/Trombe wall system using the porous medium: Experimental and theoretical study. Energy, 2019, 171: 14–26.

[10] Irshad K., Habib K., Thirumalaiswamy N., Implementation of photo voltaic trombe wall system for developing non-air conditioned buildings. 2013 IEEE Conference on Sustainable Utilization and Development in Engineering and Technology (CSUDET), 30-31 May 2013, Selangor, Malaysia.

[11] Irshad K., Habib K., Thirumalaiswamy N., et al., Performance analysis of photo voltaic trombe wall for tropical climate. Applied Mechanics and Materials, 2013, 465–466: 211–215.

[12] Irshad K., Habib K., Thirumalaiswamy N., Performance evaluation of PV-trombe wall for sustainable building development. Procedia Cirp, 2015, 26: 624–629.

[13] Huang J., Xi C., Yang H., et al., Numerical investigation of a novel vacuum photovoltaic curtain wall and integrated optimization of photovoltaic envelope systems. Applied Energy, 2018, 229: 1048–1060.

[14] Luo Y., Zhang L., Liu Z., et al., Numerical evaluation on energy saving potential of a solar photovoltaic thermoelectric radiant wall system in cooling dominant climates. Energy, 2018, 142: 384–399.

[15] Yang H., Ji J., Study on the influence of BIPV on building wall heat gain. Acta Energica Sinica, 1999(3): 270–273.

[16] Yang H., Burnett J., Jie J., Simple approach to cooling load component calculation through PV walls. Energy & Buildings, 2000, 31(3): 285–290.

[17] Jimenez M.J., Madsen H., Bloem J.J., et al., Estimation of non-linear continuous time models for the heat exchange dynamics of building integrated photovoltaic modules. Energy & Buildings, 2008, 40(2): 157–167.

[18] Friling N., Jimenez M J., Bloem H., et al., Modelling the heat dynamics of building integrated and ventilated photovoltaic modules. Energy & Buildings, 2009, 41(10): 1051–1057.

[19] Xie S., Research on thermal performance of new-type photovoltaic breathing outer wall. China University of Mining and Technology, 2017. (in Chinese)

[20] Chen X., Huang J., Zhang W., et al., Exploring the optimization potential of thermal and power performance for a low-energy high-rise building. Energy Procedia, 2019, 158: 2469–2474.

[21] Incropera F.P., DeWitt D.P., Introduction to heat transfer, thirded. John Wiley and Sons Inc., United States, 1996.

[22] Iu I.S., Experimental validation of the radiant time series method for cooling load calculations. University of Macau, China, 1999.

[23] General principles of civil building design. Ministry of Construction of the People's Republic of China, Beijing, China, 2005.

[24] Zhang Q., Yang H., Manual of standard meteorological data for building. China Construction Industry Press, 2012. (in Chinese)